Experimental research on a hydrodynamic thrust bearing with hydrostatic lift pockets: Influence of lubrication modes on bearing performance

Jean Bouyer, M. Wodtke, Michel Fillon

Version of Record: https://www.sciencedirect.com/science/article/pii/S0301679X21004011
Manuscript_9a3129e1eb212e7005308634640c9287

Experimental research on a hydrodynamic thrust bearing with hydrostatic lift pockets: Influence of lubrication modes on bearing performance

J. Bouyer [1], M. Wodtke [2], M. Fillon [1]

[1] *Pprime Institute, CNRS – University of Poitiers – ISAE ENSMA, UPR 3346, Mechanical Engineering and Complex Systems Dept., SP2MI, 11 Bd. Marie & Pierre Curie, TSA 41123, 86073 Poitiers Cedex 9, France.*

[2] *Gdansk University of Technology, Faculty of Mechanical Engineering and Ship Technology, Narutowicza 11/12, 80-233 Gdansk, Poland.*

Keywords: Thrust bearing, experimental, hydrodynamic, hydrostatic lift

Abstract

The aim of the study is to investigate the performance of a thrust bearing equipped with hydrostatic lift pockets under different lubrication modes. Three types of flat land bearing lubrication modes are studied experimentally: hydrostatic lubrication (HS; forced oil injection to the pockets), hybrid lubrication (HS+HD; hydrostatic lubrication combined with the external forced bearing oil supply) and hydrodynamic lubrication (HD; external forced bearing lubrication acting alone). Tests are performed for steady and transient states of bearing operation. The obtained results confirmed that the load-carrying capacity of the flat land bearing is poor, and the introduction of hydrostatic lubrication improves its performance. The speed is found to be a critical parameter: as it increases, the hydrostatic effect is affected and the film thickness is reduced.

1. Introduction

Hydrodynamic bearings are widely used in many machines and in many industries due to a number of advantages over other bearing types, e.g. self-acting, low losses or simplicity of construction. However, one of the problems of their operation is the limited load capacity at low sliding speeds and the unavoidable contact of the sliding surfaces during starting and stopping of the machine, which in the most unfavorable case may lead to intensive wear and even to catastrophic failure of the bearings. One of the methods used to eliminate the reduced load-carrying capacity (LCC) of hydrodynamic bearings is the use of hydrostatic jacking systems of the bearing starts and stops.

Hydrostatic lubrication is characterized by the supply of the oil under high pressure, through a lubricating pocket machined on the sliding surface, to the oil film using an external pressure system. This type of lubrication is characterized by a lack of wear for mating surfaces, has low friction losses, high stiffness and damping, as well as the ability to operate under conditions of a parallel oil gap or low or zero speeds. For this reason, hydrostatic bearings have been widely used in the construction of various machines, such as telescopes, ball mills, machine tools, precise spindles and many others [1]. Additionally, there are analytical methods that use the solution of the Reynolds equation, allowing for reliable determination of the operating parameters of hydrostatic bearings with simple shapes [2]. The disadvantage of hydrostatic lubrication is the need to use a relatively complex supply system, especially for multipad bearings. In this case, for proper operation, an independent power supply to each of the hydrostatic pockets is required or, when using one pump, application of the

flow restrictors for each oil pocket, or as in the case of opposite bearings, special self-regulating design [3]. The hydrostatic recess on the bearing sliding surface influences the phenomena in the lubricating film. Braun et al. [4,5] investigated the influence of the pocket shape and its depth on the flow pattern in the hydrostatic bearing taking into account shaft rotation. The obtained results indicate a clear influence of the chamber depth on the flow pattern in the pocket and the occurrence of irregular pressure distribution in the chamber, e.g. the existence of peaks and drops in the vicinity of the pocket ends depending on the operating conditions and the direction of shaft movement. An irregular pressure profile in the hydrostatic pockets is also confirmed by the results of tests carried out for large thrust bearings of machine tools [6]. Due to the deformation of the supporting structure of such bearings caused by high loads and high sliding speeds (160 rpm, OD 3500 mm), the oil gap thickness varies across the radial direction [7,8]. Tests of a water-lubricated high-speed hydrostatic thrust bearing (17.5 krpm, OD 76.2 mm) with a flat sliding surface indicate a negligible effect of speed on the measured film thickness [9,10]. This proves the limited participation of the hydrodynamic effect in the carrying of the load by the tested bearing. One possibility to increase the LCC of a nominally parallel gap flat land thrust bearing is to use grooves with an optimized shape on the sliding surface [11].

The common use of hydrostatic lubrication systems can also be used for active or controlled lubrication of bearings [12,13]. It is possible to influence the static and dynamic parameters of the bearings by an appropriately controlled oil supply through pockets to the oil film. The hydrostatic effect can also be achieved without the presence of a pocket at the sliding surface by using magneto-rheological fluid as a lubricant and activating an appropriate magnetic field [14]. Hydrostatic bearings and various aspects of their operation have been the subject of many studies, a summary of which can be found in recently published studies [15,16].

In the case of a hydrodynamic bearing with an activated hydrostatic assistance (hybrid lubrication), both hydrostatic (in the pocket) and hydrodynamic (a part of the pocket) effects contribute to the bearing's LCC. The proportions between the influence of both modes of lubrication on the pressure distribution in the bearing and other bearing parameters depend on the operating conditions, i.e. the rotational speed, the oil flow rate to the pocket and the load. Chaomleffel et al. [17] confirmed in experimental studies that in the case of hybrid lubrication of a lightly loaded journal bearing (eccentricity <0.4), the measured pressure distribution was similar to the distribution obtained under the hydrostatic mode of lubrication. Under higher loads, the pressure distribution changed. Due to the increased contribution of the hydrodynamic effect, there was an increase in the oil pressure between the lubrication pockets.

De Pellegrin et al. [18] investigated theoretically the influence of three shapes of the annular pockets of the same surface on the performance parameters of the hybrid lubrication of a tilting-pad thrust bearing with spring support. The calculated operating parameters of the bearing (e.g. minimum film thickness) differed strongly depending on the analyzed pocket shape. Additionally, it was found that with the increase of the rotational speed, the presence of the pocket degrades the operating parameters of the bearing compared to the case of the pad without pocket. This effect is especially important for hydrodynamic bearings equipped with a hydrostatic jacking system for starting and stopping, e.g. the large size tilting-pad thrust bearings of water turbines [19]. The results of experimental tests confirm that the pocket of these bearings (usually not supplied with oil after reaching the appropriate sliding speed) significantly disturbs the pressure profile of the hydrodynamic film [20–22]. It is advantageous to use relatively shallow pockets, because they have the smallest impact on the hydrodynamic pressure profile and, consequently, on reducing the bearing LCC [23,24]. Moreover, it has been shown that with the increase in the size of the hydrostatic chamber, the margin of safe operation of the bearing decreases in the regime of hydrodynamic operation [23,25] (with thinner films or lower LCC calculated compared to a pad without pockets). In

the case of tilting-pad thrust bearings with symmetrical support in the circumferential direction, a large size of lubricant pocket may also adversely affect the inclination of the segment in the wrong direction during bearing startup [26]. For these reasons, the size of the lubrication pockets of hydrodynamic bearings with hydrostatic jacking systems should be as small as possible; however, their minimum size is limited by the value of the maximum oil pressure necessary to separate parts and form a hydrostatic film [18].

The presented literature review confirms that many aspects of the oil lubricated bearings equipped with the hydrostatic jacking system have been investigated. However, detailed comparative studies of different modes of lubrication for thrust bearings have not been an object of research so far. The main goal of this paper is to investigate experimentally the operational parameters of a thrust bearing under three modes of lubrication, namely: hydrostatic (HS), hybrid (combined HS + HD) and hydrodynamic (HD). To fulfill the goal of this research, a dedicated test stand was adopted. A flat land thrust bearing equipped with hydrostatic pockets was selected as the object of analysis. Detailed measurements of the pressure and temperature fields on selected bearing pads as well as of the film thickness and the bearing friction torque allowed comparison of the bearing performance under the different modes of lubrication studied. The tests cover steady and transient states of bearing operation.

2. Materials and Methods

The test rig used in this work was the thrust bearing test device at Pprime Institute. This test rig was designed in the 1990s, and has been modified many times to incorporate the newer measurement technologies that have become available. Extensive work has been done on several types of bearings, including both tilting-pad and fixed geometries. Harika *et al.* [27] studied the influence of the presence of water in oil on the performance of a tilting-pad thrust bearing. Later, Henry *et al.* [28–30] conducted an extensive study of the performance of a textured parallel flat thrust bearing and compared it to classically designed bearings. Since this test rig was extensively described in these previous works, we will only describe the main operating parameters and devices here that are specific to this study.

It should be noted that the thrust bearing used in this study has exactly the same dimensions as that used by Henry *et al.* [28–30]. A general schematic of the test rig is shown in **Fig. 1** a. It consists of a rigid frame with a high precision spindle, with a collar driven by a 15 kW DC motor at speeds varying from 0 to 10000 rpm with an accuracy of +/-20 rpm. The test cell faces the collar in the upper part of the rig, where loading takes place. A hydraulic system permits the bearing to be fed with oil at constant pressure and temperature with an embedded precision PID controller.

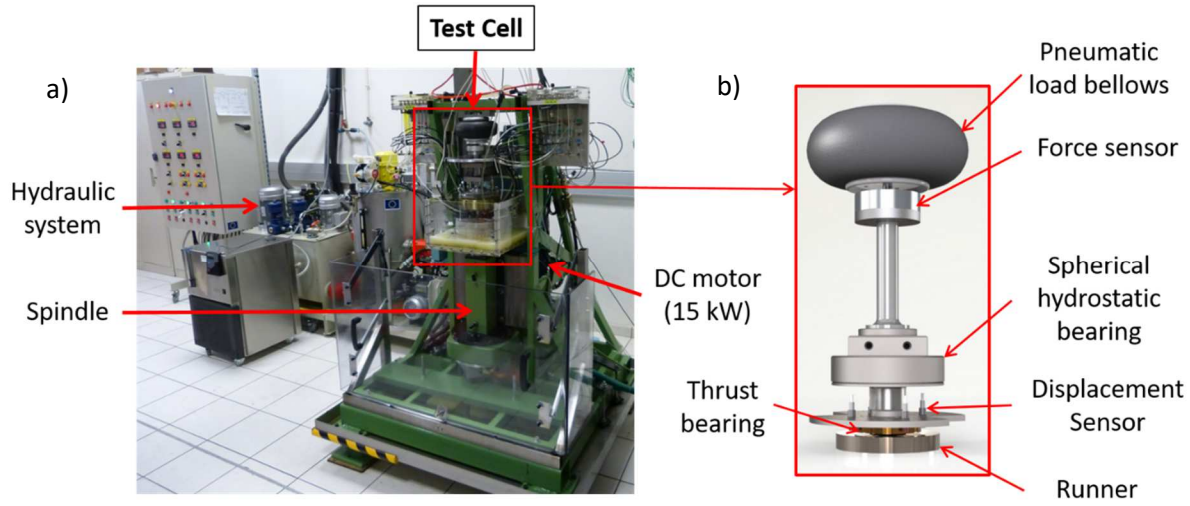

Fig. 1. Thrust bearing test rig; a) general view, b) details of the test cell

Fig. 1 b presents a detailed view of the test cell. The load is applied vertically by means of a pneumatic jack, which is electronically controlled and supports a maximum load of 8000 N. The maximum uncertainties in the loading system are within +/-20 N. The load (measured by a force transducer) is transmitted to the test bearing by means of an arm and a spherical hydrostatic bearing, which is connected to the bearing support and enables correct alignment of the surfaces of the bearing and runner by unconstraining the rotational degrees of freedom. The bearing therefore has three rotational degrees of freedom and one translational degree of freedom, i.e. the direction of the load. The rotation of the bearing is prevented by a finger in contact with a load cell, thus allowing direct measurement of the torque induced by the shear of the oil in the oil film gap during rotation. The test rig was also equipped with a tachymeter to measure the shaft speed and a flowmeter for the oil supply.

The relative displacement of the bearing versus the runner was measured using five eddy current displacement sensors, four of which were placed at 90° from each other around the outer diameter of the bearing and one in the center. The measurement results of the film thickness presented here are those from the central sensor, since this probe was found to have a higher stability than the outer ones. Since eddy current sensors are very sensitive to the target they face, the outer sensors provided measurements with discrepancies that were too high compared with the central one, which always faced the same target. The film temperature was measured with type K thermocouples with diameter 0.25 mm, whose tips had direct contact with the oil film, since they were placed in the open holes drilled across the bearing thickness. The global accuracy of the temperature was well within +/-0.5 K, taking into account slight variations in load and speed. The pressure transducers used within the research were of a wet-type strain gauge design. They were connected by elastic pipes with the holes drilled across the bearing (the same pattern as the temperature points) by threaded slots with the collector (fixed to the bearing back, each pressure line sealed separately). The pressure and temperature measurements at the film–bushing interface were performed simultaneously by a National Instruments DAQ system with signal conditioning, which was also used for command and control of the test rig. Details of the sensors (types, accuracy, ranges) applied within the present research were given in papers [27–31].

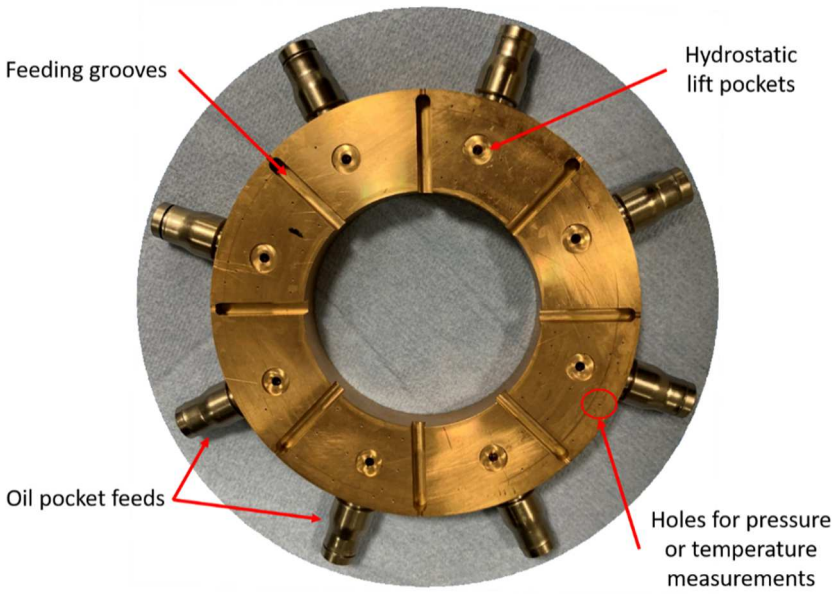

Fig. 2. View of the sliding surface of the tested bearing.

The thrust bearing tested was a fixed geometry planar bearing comprising eight pads (flat lands parallel to the runner surface), all of which were equipped with identical hydrostatic lift pockets 6 mm in diameter (**Fig. 2**) and with a depth of 0.4 mm. The supply to the bearing depended on the condition being tested. When operating in the classical hydrodynamic mode (HD), the lubricant was supplied to the bearing only from its center by means of deep grooves ending in gouges. When the hydrostatic mode (HS) was selected, the bearing was no longer fed by the center but solely by the lift pockets at constant pressure. The last series of tests was made with both supply conditions, i.e. hydrostatic and hydrodynamic (central supply) at the same time (HS+HD). In order to ensure good equilibrium of the hydrostatic pressure (when used), all the oil pressure feeds were interconnected with tubes, and each oil feed was equipped with a non-return valve to prevent hydrodynamic pressure being exerted back towards the feeding system. The hydraulic system allowed for constant temperature and pressure of the feeding oil to be maintained, at 40°C and within 2–2.5 bar, respectively, which obviously varied slightly with the load. The corresponding flow rates were 2 l/min for the central supply and 2.25 to 2.85 l/min for the hydrostatic supply.

The bearing and lubricant characteristics are given in **Table 1**. The materials used for the tested thrust bearings were bronze UE9P for the thrust pads and steel XC38 for the runner. As shown in **Fig. 3**, the temperature field was measured using 32 thermocouples. Two opposite bearing pads were equipped with a set of 24 thermocouples (sensors marked **T9** – **T20** in pad #4 and **T21** – **T32** in pad #8). An additional 8 thermocouples (**T1** – **T8**) were installed at the standard 75%-75% relative position along the radial and circumferential dimensions of each pad. Twelve thermocouples in two selected bearing pads were placed in sets of four at 11%, 40%, 69%, and 82% of the relative pad circumferential length and at three different radiuses corresponding to 15%, 50%, and 85% of the relative pad width. The pressure field was monitored with eight pressure measurements inside the pockets located near the trailing edge (sensors marked **P1** – **P6**), and 11 others (**P18** – **P28**) were spread over pad #6, at angular and circumferential positions identical to those used for the temperature measurements.

Table 1. Characteristics of the bearing and lubricant

Parameter	Symbol	Value

Number of pads	N_p	8
Outer diameter	D_{out}	90 mm
Inner diameter	D_{in}	50 mm
Pad thickness	Th_p	10 mm
Groove depth	D_G	4 mm
Groove width	W_G	3 mm
Hydrostatic pocket diameter	D_p	6 mm
Hydrostatic pocket depth	W_p	0.4 mm
Hydrostatic pocket relative positions (radial / circumferential)		50% / 58%
Lubricant		ISO VG 46
Viscosity at 40°	μ_1	0.0416 Pa.s
Viscosity at 80°	μ_2	0.0105 Pa.s
Lubricant density at 20°	ρ	865 kg/m^3

The bearing sliding surface accuracy was required to be less than 10 µm of flatness error as well as parallel error relative to the bearing back surface. To confirm that, the surface of the bearing was controlled before testing by means of a contacting flatness measurement device (Talyrond 365 from Taylor Hobson), which rotates the bearing and measures its flatness precisely along several radii. The flatness was measured along 12 different radii from the inner to the outer diameter. Only small differences were noticed between those measurements, and the flatness profile did not vary significantly as a function of the radius. It was thus decided to present in **Fig. 4** the results obtained for one radius (40 mm) where the pressures and temperatures should show their maximum values.

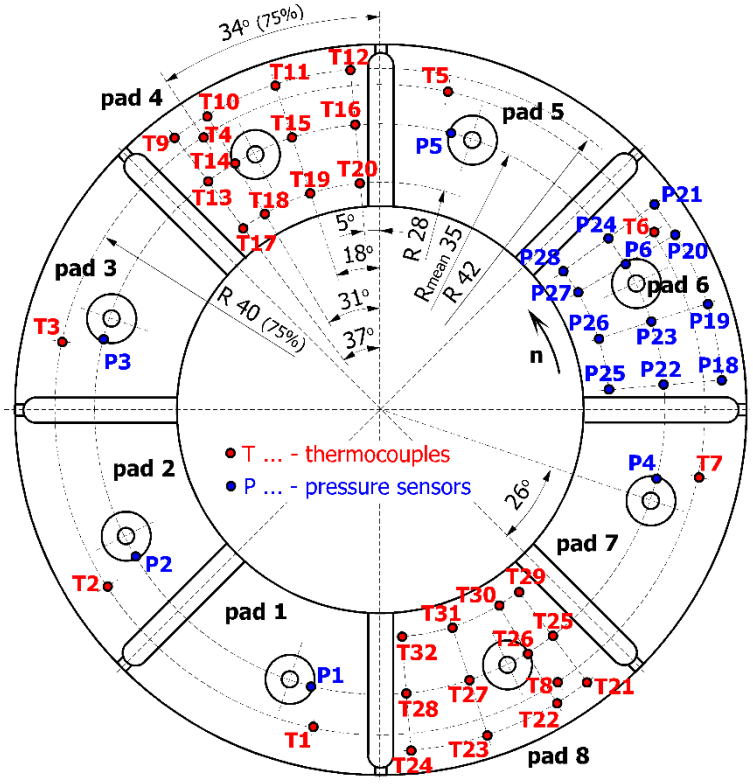

Fig. 3. Arrangement of the temperature and pressure sensors in a tested thrust bearing.

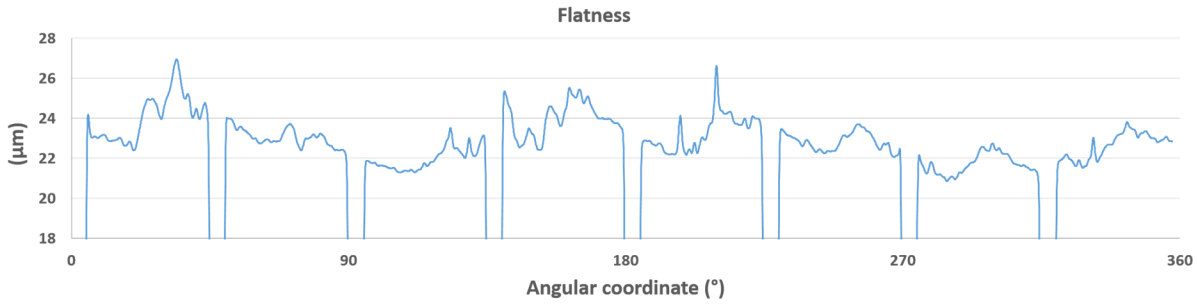

Fig. 4. Flatness measurements at 40 mm bearing radius.

As shown in **Fig. 4**, some discrepancies between the pads were found when the flatness of the bearing was measured. When adjacent pads were compared, the highest difference was 3 µm, and for all pads, this difference did not exceed ± 3 µm. However, this could significantly influence the bearing behavior, especially in cases where the film thickness is very small.

3. Experimental results and discussion

In order to ensure a high level of repeatability of the results, each test was repeated at least three times. A constant feed temperature was maintained for all tests (40 ± 0.2°C). Singular steady state measurement at the defined speed and load level took about 30 s, and the parameters were recorded with the 4 Hz frequency. For transient states tests (starts / stops) a higher frequency of the bearing parameters recording was applied (50 Hz). Errors of measurements were discussed in papers [27–30].

The results presented below are an average of the data obtained in each series of tests. Measurements were taken for three lubrication modes under the following operating conditions:

(i) HS+HD (hybrid lubrication, oil supplied to the bearing by pockets and central supply line); speed varying from 0 to 8000 rpm and load between 500 and 2500 N;

(ii) HS (hydrostatic lubrication, oil supplied to the bearing by pockets only); with speed varying from 0 to 8000 rpm and load between 500 and 2000 N;

(iii) HD (hydrodynamic lubrication, oil supplied to the bearing by central supply line only), with speed varying from 0 to 4000 rpm and load between 500 and 1000 N.

The increments used were 2000 rpm for the speed and 500 N for the load. It was not possible to test the bearing under different modes of lubrication in the same range of imposed operating conditions because of two reasons. In the case of the HS and HS+HD modes of operation, the limitation came from the equipment utilized. It was not possible to reach a pressure in the hydrostatic supply system higher than ~1.7 MPa (due to the strength of the elastic pipes used to divide the oil from the pump to the pockets through non-return ball valves). Under the HS mode of operation, the pressure in the oil film was slightly higher than in the HS+HD case. For that reason, the range of allowable operating conditions that it was possible to obtain for the HS mode of lubrication was narrower than in the case of the HS+HD mode (it was not possible to obtain loads higher than 2000 N). The other limitation is connected with the safety of the bearing operation. It was revealed that under the HD mode of lubrication very thin oil films were measured, even under relatively low loads and small speeds.

Startup and stop tests were also conducted after the steady-state tests. Since a large number of operating conditions were tested, we report and discuss only the most significant here. The

remainder of this section is divided into two subsections that consider steady-state operation and the transient startup/stop conditions.

Steady-state operation

The first results presented here are the global parameters characterizing the performance of the thrust bearing, such as the film thickness, friction torque, and temperature at the 75%-75% position. It should be noted that, since the lubrication theory gives no load-carrying capacity for the flat thrust bearing, only cases of low load were tested with the HD lubrication mode, to prevent any damage to the bearing. The figures are presented in three columns representing the three lubrication modes.

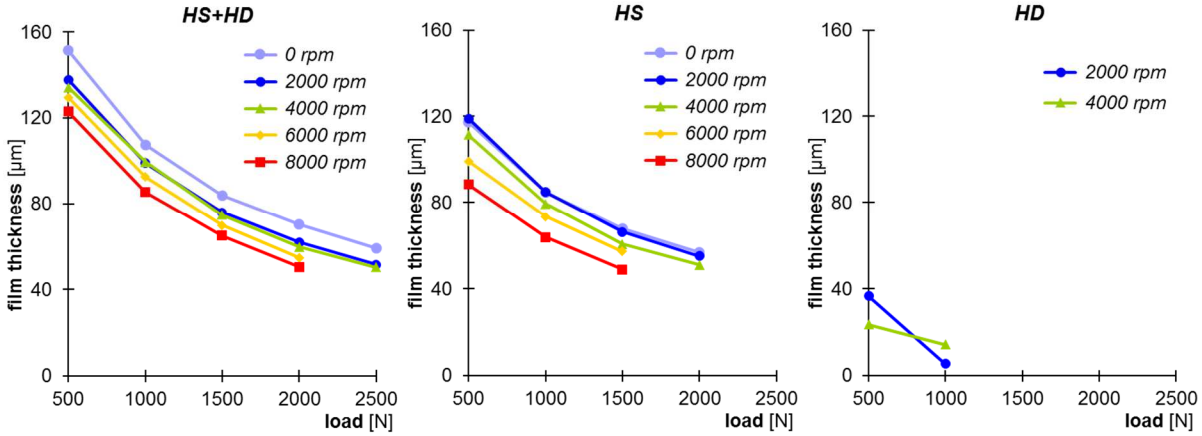

Fig. 5. Film thickness measured by the central sensor.

Fig. 5 gives an overview of the results obtained for loads between 500 and 2500 N and speeds from 0 to 8000 rpm. The film thickness provided by the flat land thrust bearing operating in HD mode is very small (less than 40 µm under 500 N). On the other hand, for the HS case, the film thickness persists until either the load or speed is too high to maintain good hydrostatic lubrication. At a load of 500 N, the film thickness is constant at 120 µm at speeds of up to 2000 rpm. The increase in speed leads to a decrease in the film thickness to values of 111, 99 and 88 µm at 4000, 6000 and 8000 rpm, respectively. This clearly proves that the higher the speed, the greater the influence of rotation on the hydrostatic oil film, as it is reduced by more than 25% between 2000 and 8000 rpm. However, the influence of the load is also significant, and causes the film thickness to decrease by more than 27% when the load is increased to 1000 N. At 1500 N, the film thickness continues to decrease by about 20%. For higher loads, the film thickness decreases again, and for an increase in speed up to 8000 rpm, the behavior of the bearing under hybrid lubrication (HS+HD) reveals that there is a hydrodynamic film that partially compensates for the decrease in the film thickness. At a high speed of 8000 rpm, the film thickness is 123 µm at 500 N (40% higher than with HS alone), but this is still reduced by 30% at 1000 N to 85 µm. In the case of flat land parallel surfaces, the hydrodynamic effect is limited and occurs only in the case of surface deviations (elastic, geometric or thermal), which is why its contribution to the overall load capacity is rather small. In addition, thicker oil films in the case of HS+HD are connected with a larger oil volume flowing through the bearing (oil injected to the pockets and supplied by the central hole are summed). The impact of the load is clearly significant, and this is due to the fact that the hydrostatic lift pockets were dimensioned for low loads. A higher hydrostatic feeding pressure could also compensate for this effect. Generally, it is expected for hydrodynamic bearings that the oil film thickness increases with increase of the sliding speed. The results obtained for the HD mode of bearing operation revealed, unexpectedly, that the measured oil film thickness was thinner at 4000 rpm than at 2000 rpm (for 500 N, see **Fig. 5**). This is probably due to the influence of thermal bearing deformations, which, together with possible

deviations of the bearing's initial geometry, could unfavorably change the oil film profile when the speed increased. In addition, the presence of the pockets manufactured on the bearing's sliding surface introduced discontinuity of the geometry (and oil film), which is very unfavorable for the hydrodynamic effect.

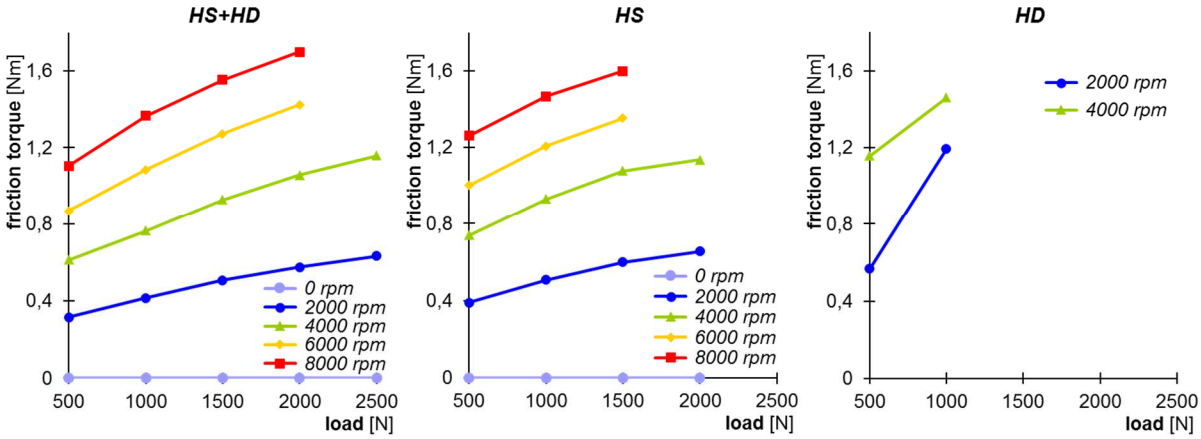

Fig. 6. Friction torque.

The behavior of the friction torque presented in **Fig. 6** is classical, as it increases as a function of the speed. As expected, the higher the speed or the load, the higher the friction torque. However, the most significant effect is that of the speed, since higher speeds provide higher shearing of the lubricating layer and consequently greater losses. Comparing all the tested bearing lubrication modes, the smallest friction torques at certain operating conditions were measured for the hybrid mode. The measured friction torques for the hydrostatic mode were only slightly higher than under hybrid lubrication. This is due to the lower oil film thickness and thus higher shearing gradients in the gap (at a similar level of the oil film temperature and thus viscosity, see **Fig. 7** - **Fig. 9**). The highest losses were measured under hydrodynamic lubrication of the bearing, but it should be noted that this is perhaps due to the unfavorable impact of the hydrostatic pocket.

The evolution of the maximum temperature measured at 75%-75% is shown in **Fig. 7**. It should be recalled that each bearing pad is equipped with one thermocouple placed at 75%-75%, as mentioned in Section 2; the discrepancies between the values recorded at the eight thermocouples generally do not exceed 2 K, except for the high-speed case, where they can reach 5 K. Bigger discrepancies of measured temperatures were observed for higher speeds and consequently for slightly lower oil film thicknesses (see **Fig. 5**). In such operating conditions, larger friction due to oil shearing in the gap is generated. This is due to the fact that differences in the oil film thickness between individual bearing lands (due to flatness error of the bearing's sliding surface, **Fig. 4**) resulted in more visible differences in the obtained temperatures.

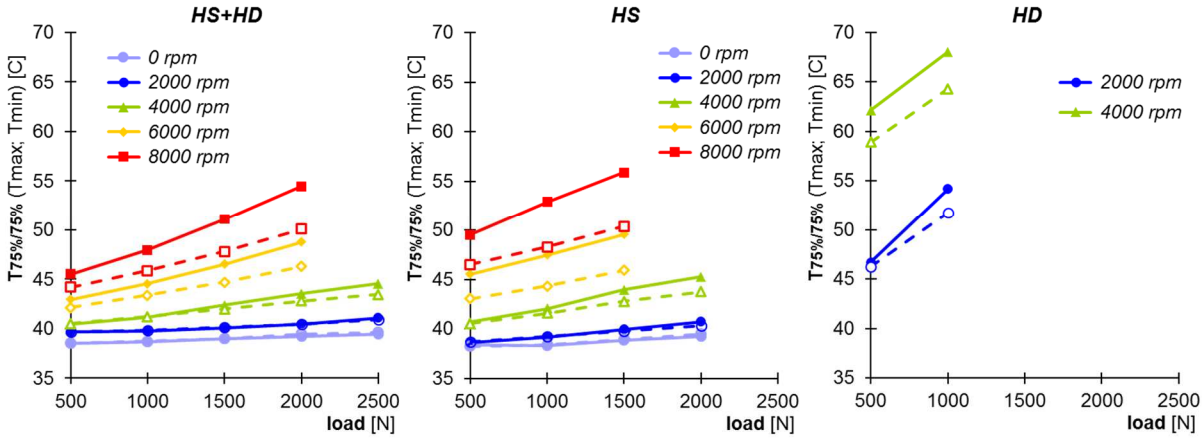

Fig. 7. Maximum (solid line) and minimum (dashed line) values of the temperature given by the 75%-75% thermocouples.

As expected, the temperature increases as a function of speed due to the higher shear in the oil film for all the cases tested here. For low speed (2000 rpm), the measured temperature rise with the increase of the load is relatively low for the HS+HD and HS cases. Together with the increase of the speed, the measured temperature rise in the bearing is higher when compared to the lowest speed. It can be noted that, under the HS mode of lubrication, the bearing operates in conditions of slightly higher temperature than under the HS+HD mode. This is due to the larger volume of oil flowing through the bearing. In the case of the HD mode of lubrication, the increase of the bearing temperature with the load for constant speed was measured as the highest for all the tested configurations. In this case, both friction and temperature are significantly increased probably due to partial contacts in the bearing. If we look at what happens at the mean radius for the 1000 N load shown in **Fig. 8** (upper row), we can make the same observations: the highest temperatures are obtained in the HD mode due to high friction, even if the speeds are low. Comparison of the measurements made at pads #4 (solid line) and #8 (dashed line) shows that the shapes differ significantly at 70% of the pad angle - this is the location of the thermocouples inside the pockets (T14 and T26). This difference can be explained by the fact that these thermocouples were placed manually and may not have the same positions relative to the film. Nevertheless, the fact that they were placed inside the pockets put them relatively far from the lubricating film, and they in fact measured a combination of the temperatures of the fluid film and the fluid inside the pocket.

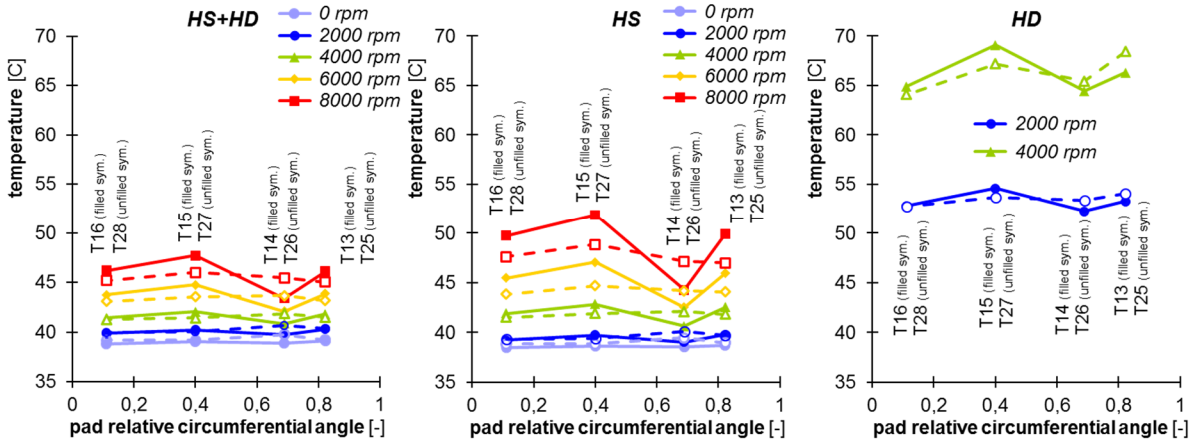

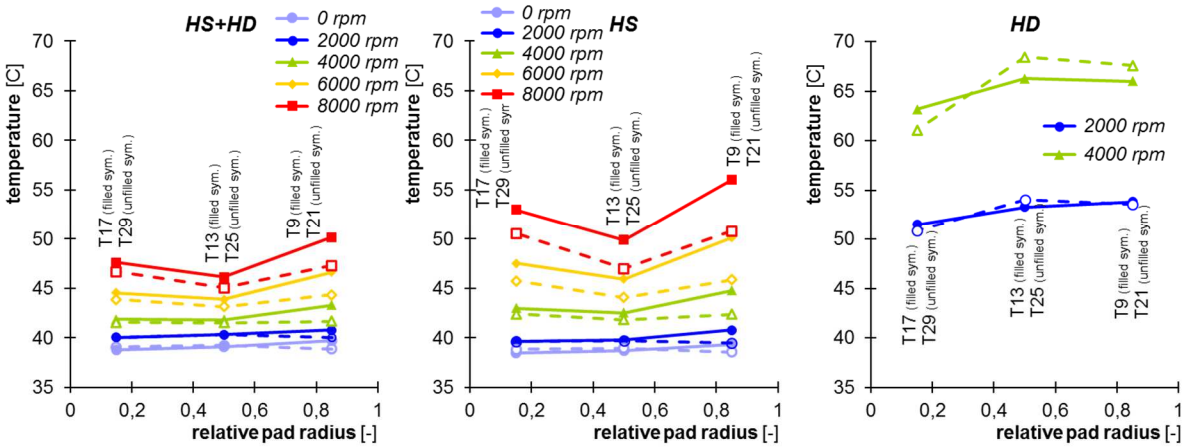

Fig. 8. Recorded temperatures on pad #4 (solid lines) and pad #8 (dashed lines) for a load of 1000 N: circumferential at mean radius (upper row) and radial close to the trailing edge (lower row).

In the lower row of **Fig. 8** the measured radial temperature profiles of the instrumented pads close to the trailing edge are shown. For the hybrid and hydrostatic lubrication modes at a speed of 2000 rpm only a small temperature increase from the bearing's inner to outer radius was recorded. At higher speeds, this temperature rise was not continuous and the measured temperatures were the smallest on the mean bearing radius (thermocouples T13 and T25). This is a result of supplying the oil into the pockets at a temperature lower than the oil film. Cold oil from the pockets, due to rotation of the collar, is forced towards the trailing edge, resulting in lower temperatures on the mean bearing radius compared to the inner and outer bearing radii. This effect is not visible in the case of the HD mode, and the recorded radial temperature profile at the trailing edge is typical for a hydrodynamic bearing.

Increasing the load up to 2000N, as shown in **Fig. 9**, leads to a sharp increase in temperature due to the large reduction in the film thickness; however, all the trends observed at the lower load were also visible. It was therefore not feasible in those tests to operate the bearing with HD only, since the hydrostatic lift effect is essential to create a lubricating film. Moreover, under the HS condition, it was only possible to reach this load at lower speeds, due to the limitations on the test rig discussed earlier.

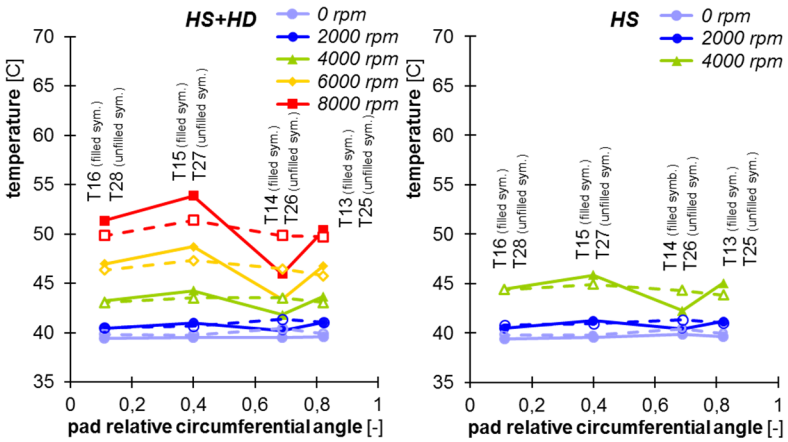

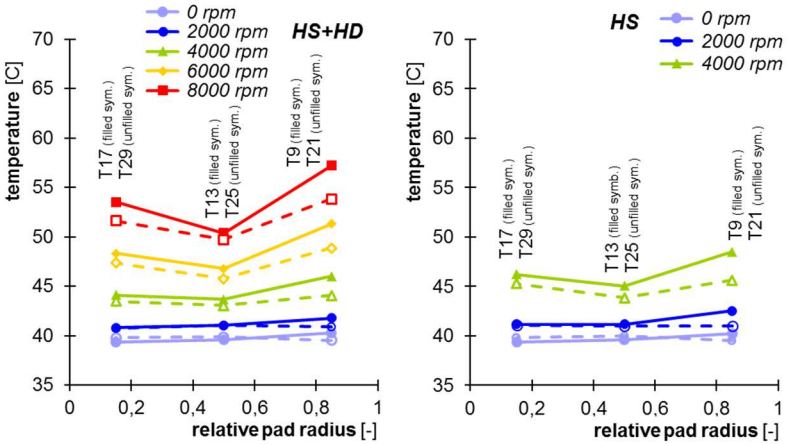

Fig. 9. Recorded temperatures on pad #4 (solid lines) and pad #8 (dashed lines) for a load of 2,000 N: circumferential at mean radius (upper row) and radial close to the trailing edge (lower row).

By comparing the results in **Fig. 8** and **Fig. 9** for the HS+HD condition, we can see that the temperature globally increases by 5 K and even up to 7 K at 8000 rpm. For the HS condition, the speed is lower and the temperature increase is weaker: 2 K and 3 K at 2000 and 4000 rpm, respectively. It can also be noticed that highest temperatures for all of the presented results were measured for the HD mode of bearing lubrication, even when operated under lower speed and load than other tested modes of bearing lubrication.

Fig. 10 shows the pressure measurements inside six pockets, where the two other pockets were equipped with thermocouples instead of pressure measurements. The pressure increased with the speed by between 15% and 30%, depending on the supply mode. It can be seen that the measurements on all of the pads were similar for both the HS+HD and HS modes, but slightly higher pressures were recorded for the HS mode. Under the HS+HD mode, the hydrodynamic effect is very limited, but much more oil flows through the bearing (from inside to the outside) due to activation of the central oil supply. The bearing design contains closed radial grooves for lubrication of the pads. These restrict the oil flow outside the bearing, which results in slight increases of the oil pressure in the grooves and thus lower values of pressure in the pockets required to carry the exerted axial bearing load. For the HD mode, the pressure was recorded on pads #1 and #7 only. This behavior is due to geometrical defects that cause imperfect flatness of the pads. For the HS or HS+HD modes, these defects were largely compensated for by the hydrostatic feeding, while for the HD mode, only pads #1 and #7 (of those that were instrumented) were sustaining the load. This explains why the temperatures and friction were much higher in this case.

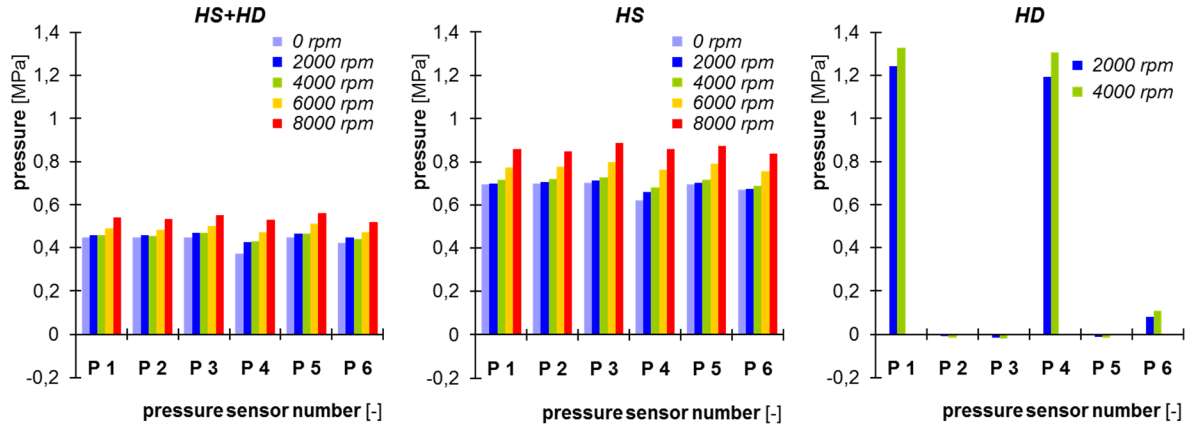

Fig. 10. Pressures recorded inside the pockets for a constant load of 1000 N.

Fig. 11 and **Fig. 12** show the oil film pressure profiles for the mean bearing radius obtained for 1000 N and 2000 N of load respectively. The dots in the figures are the measured oil film pressures while the dotted lines are the interpolated pressure profiles under the assumption that the pocket pressure is constant and equal to the pressure value inside the pocket measured by the sensor P6. The measured pressures are the maximum oil gap pressure for the HS+HD and HS modes of bearing lubrication. However, in the case of the HD mode, this is with a high probability not true, since the hydrodynamic effect will occur outside the pocket (at the nominally flat pad land which had preferable initial shape flatness error or with beneficial thermo-elastic deformations due to temperature gradients and pressure). In such a case, the maximum pressure is most likely higher and located outside the pocket. It can be seen in **Fig. 11** and **Fig. 12** that the pressure for the HS+HD and HS modes increases up to 0.7 of the circumferential relative bearing angle (pocket location) before decreasing at the trailing edge. The shape of the pressure field (for HS+HD and HS) changes slightly with the speed variation. However, because the integral of the pressure field should be equal to the applied load, together with the pressure increase with the speed at some locations (0.7) a simultaneous pressure decrease in other locations was observed (0.8). This is in liaison with the expected pressure field behavior to maintain a constant value of the integral of the pressure under operation with the constant load value.

This behavior is the same regardless of the lubrication mode. For the HS and HS+HD modes, the pressure increases with an increase in speed; however, for the HD mode, there is almost no pressure generation except in the pocket zone, which could create a small hydrodynamic pressure due to the geometrical discontinuity. It can be observed that much larger pressures were measured in this mode of bearing operation for the other selected pads (pads #1 and #7; see **Fig. 10**). This is because, for the instrumented pad used here, almost no hydrodynamic effect was present, while in some other selected pads it was measured. This can be concluded directly from the oil pressure measurements for the HD mode of lubrication presented in **Fig. 10**.

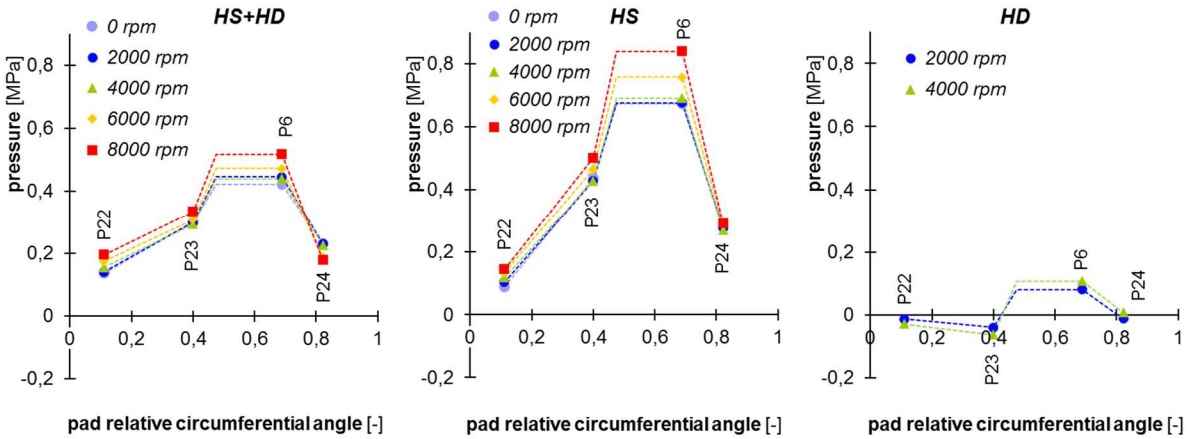

Fig. 11. Circumferential pressures recorded at the mean bearing radius for a constant load of 1000 N.

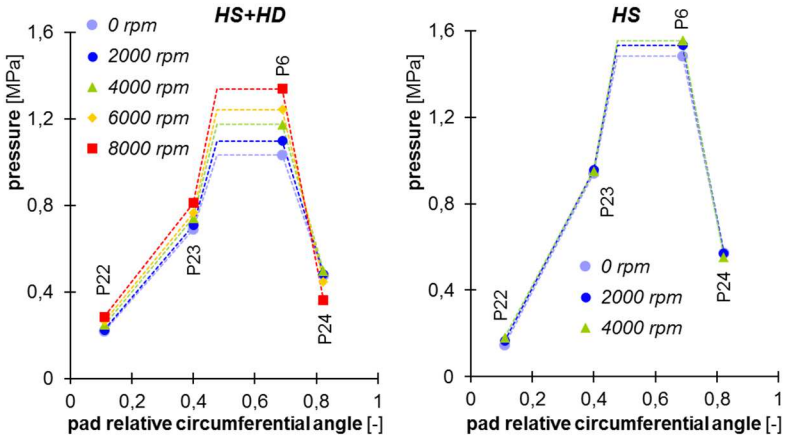

Fig. 12. Circumferential pressures recorded at the mean bearing radius for a constant load of 2000 N.

A comparison of **Fig. 11** and **Fig. 12** shows that when the load is doubled, the pressure is obviously much higher, with an increase of 143% in the maximum pressure of the HS+HD case and 120% for the HS case at 8000 and 4000 rpm, respectively.

Startup and stop

It was decided to carry out transient states bearing tests only for two configurations: HS and HD. This choice was motived by the fact that in the trial test of the HS mode of lubrication, relatively thick oil films and low friction torques were measured, without any unexpected transient effects at the startups and shutdowns. Based on the steady state results presented previously (**Fig. 5** and **Fig. 6**), only a small difference could be expected in the results of the HS+HD mode when compared to HS operation (most likely in the HS+HD configuration slightly thicker oil films and slightly lower friction torques would be measured). The parameters were measured at a high sampling rate in order to capture the rapid variations in the friction torque, which is a key parameter of the startup and stop transient modes. These periods directly influence the lifetime of the bearings, which is obviously connected with the wear that occurs in these modes. The conditions of the tests were as follows: startup from 0 to 2000 rpm in 3 s under constant load; maintain at nominal speed for a short period (~15–20 s); and free-wheel stop. Three levels of load were tested (500, 1000 and 1500 N). In the same way as for the steady-state tests, at least three repetitions were completed for each load.

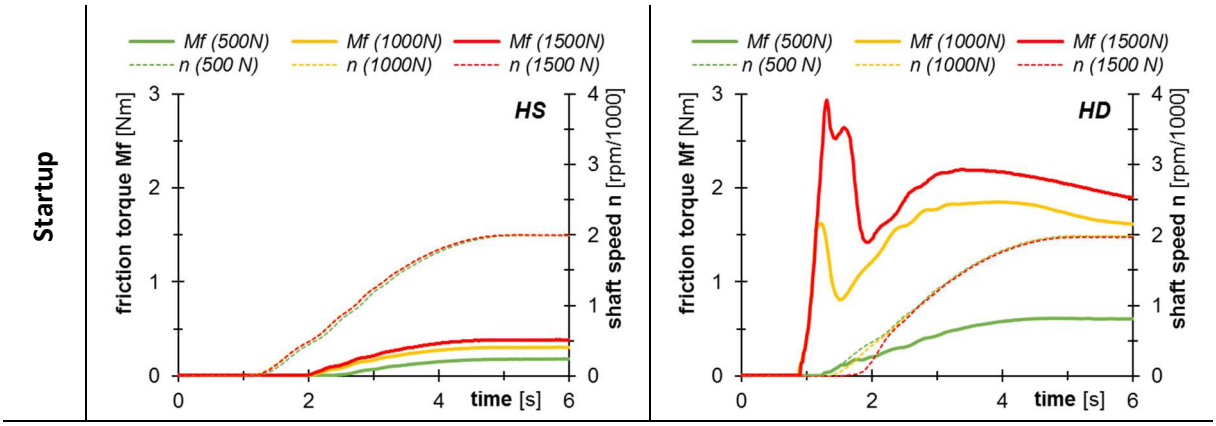

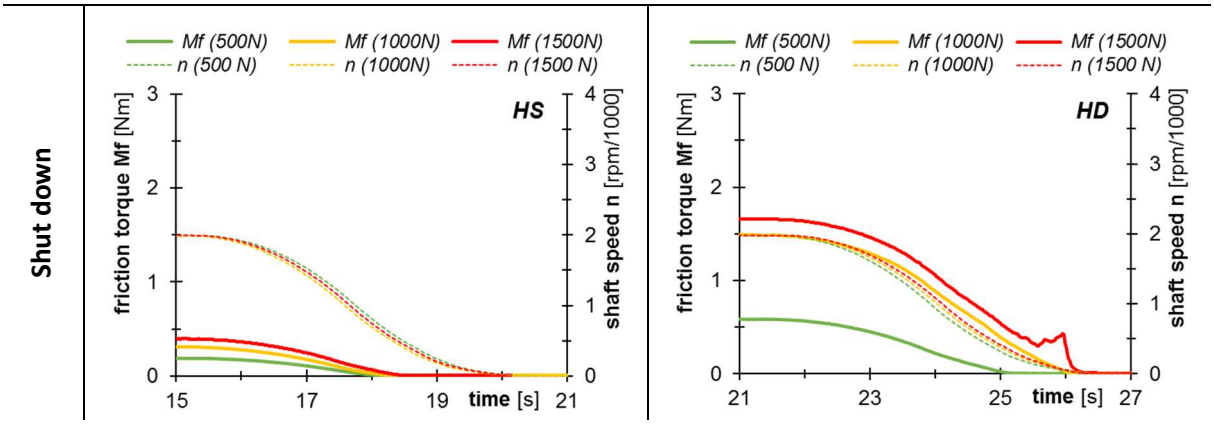

Fig. 13. Friction torque recorded at startup and shutdown for HS and HD modes of lubrication.

The left-hand images in **Fig. 13** show the behavior of the hydrostatic thrust bearing for both startup and stop in the HS mode. It can be noticed that there is no measurable friction below 200 rpm, and a slight increase is then seen with increasing speed, as the oil film is more intensively sheared by the rotation of the runner. The highest friction torque is obtained for the HD mode, as shown in the right-hand images in **Fig. 13**. For the HD mode, the behavior is close to that of a classical flat thrust bearing. The torque first increases very rapidly to a high value, due to the direct contact between the surfaces. When oil penetrates between the surfaces, the torque decreases but remains at a value that is more than three times higher than that observed for the HS mode. The friction then increases with the speed, before decreasing over time as thermal effects arise and modify the geometry of the flat bearing to generate hydrodynamic pressure. Another peak is also observed at shutdown, where the film thickness decreases due to the decrease in speed at the moment when the contact occurs between the surfaces of the bearing and the runner. This analysis is confirmed by **Fig. 14**, which shows the relative film thickness recorded by the displacement sensor placed in the center of the bearing. In the HS mode, the film thickness is almost constant, regardless of the speed, while in the HD mode, it is zero and increases with speed as soon as the oil enters the contact just after the maximum torque (see **Fig. 13**). It is worth noticing that the course of the measured friction torque for the HD mode of lubrication at the startup and shutdown is different. At startup, the initial pads geometry does not have a beneficial shape for hydrodynamic action, and mixed friction probably occurs. After the full speed is reached, intensive oil shearing and heat generation take place in the gap. Due to thermal gradients, shape deviations of the pads' sliding surface appear, which are advantageous for both fluid friction and the hydrodynamic effect. The preferable pads shape is still present when the shaft is stopping. Therefore, this results in low friction at this stage of transient bearing operation.

For the HS mode, the friction depends only slightly on the load, while for HD there is a strong influence of the axial load on losses at the startup. For the highest load, the friction torque increased the most. Simultaneously at the shutdown, there were no visible increases of the measured losses, excluding the case of the highest load, where a small friction torque fluctuation was noticed before the shaft stopped. Concerning the film thickness, significant differences between both types of the bearing lubrication modes can be identified. For the HS mode, relatively thick oil films were measured irrespective of the load (the minimum oil film was around 80 µm for the highest load). This means that the bearing worked with full film lubrication under the HS mode of lubrication irrespective of the transient state of its operation.

In the HD mode of lubrication, much thinner oil films were measured. What is interesting under the lowest load was that the obtained oil film thickness was more than 40 µm (i.e. was not equal to zero). This is because the axial bearing load was too low to remove the oil from the gap due to squeezing. The friction torque measured was of the same order of magnitude as for the HS mode of lubrication. However, when the axial load was higher (1000 and 1500 N), the initial oil film thickness

was close to zero. Together with the increase of the shaft speed, a hydrodynamic film started to develop, but its measured thickness was no higher than a dozen microns. This is likely not enough to ensure full film lubrication of the bearing under HD mode, keeping in mind bearing flatness errors.

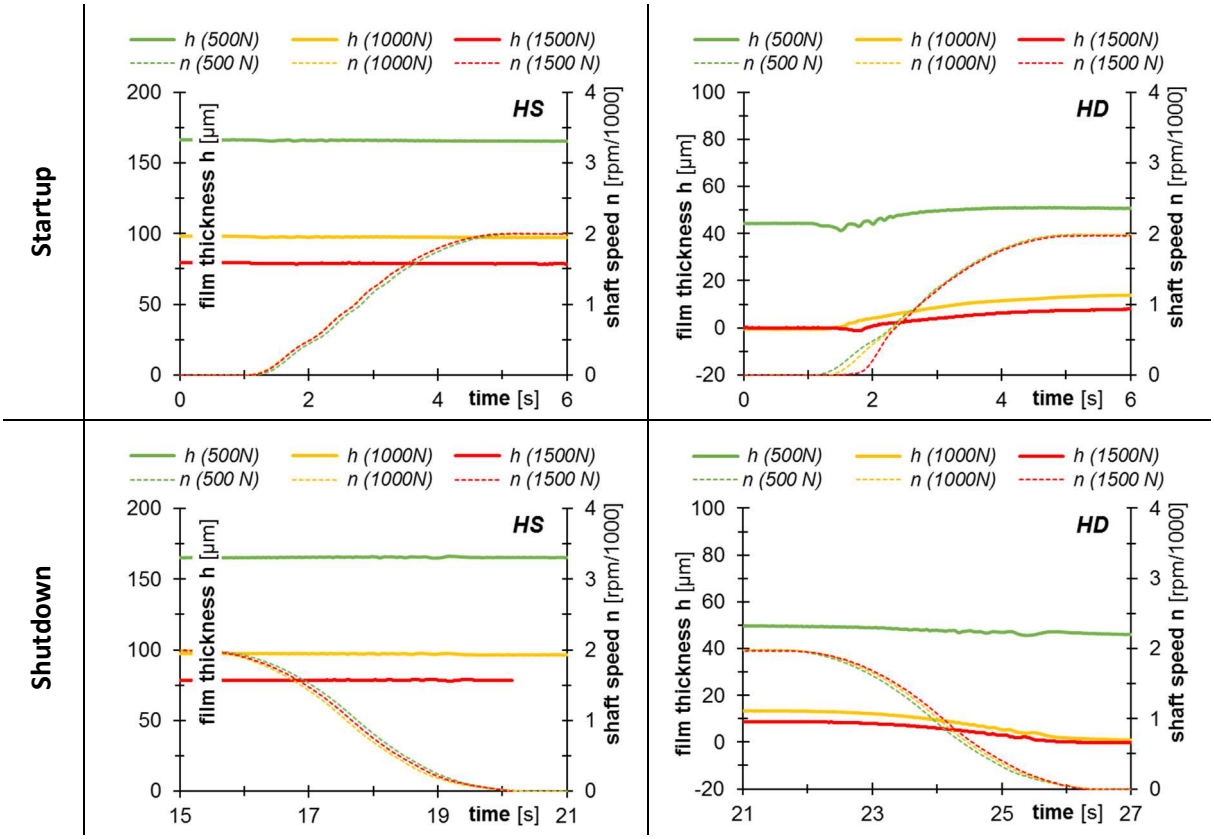

Fig. 14. Transient relative film thickness vs time recorded at startup and shutdown for HS and HD mode of lubrication.

The startup behavior of different designs of fixed geometry thrust bearings having the same size as in the present research was also an object of analysis of separate experimental research [28]. Apart from the impact of the surface texture on the starting behavior, three common bearing designs were tested, namely:

- flat land thrust bearing - the same design as in the present research (**Fig. 2**) but without pockets,
- tapered land thrust bearing – the sliding surface is composed of two sections: tapered, which is inclined along the bearing's circumferential direction starting from the oil film inlet (depth 20 µm, width 15 mm) and flat land, which is parallel to the runner surface,
- pocketed pad thrust bearing - with shallow pockets at each pad, which were connected with the inlet groove, pocket geometry: 70% of pad circumferential length (starting at the oil film inlet), 75% of the radial length (position centered radially), depth 20 µm.

A comparable testing procedure, lubricating oil supply conditions and the same oil grade and bearing testing device were used in work [28] and in the present research. This allows for reliable comparison of the startup performance of different designs of fixed geometry thrust bearings. In **Table 2** the peak values of the measured friction torque during startups for all the tested bearings are collected. This parameter is important for the lifetime of the bearing.

Table 2. Measured friction torque peaks during startup for different designs of the fixed geometry thrust bearings.

Thrust bearing design	Load [N]		Lubrication mode	Source of results
	1000	1500		

Flat land	2.9 Nm	5.9 Nm	HD	[28]
Tapered land	3.2 Nm	7.0 Nm		
Pocketed	1.8 Nm	3.6 Nm		
Flat land with pockets	1.6 Nm	3.0 Nm	HD	present study
	0 Nm	0 Nm	HS	

The results confirm the obvious fact that the best performance during startup (in terms of friction torque) is obtained from the flat land bearing with pockets under the hydrostatic mode of lubrication (friction torque peaks are not present at all, **Fig. 13**). Surprisingly, for the flat land bearing with pockets under the HD mode of lubrication, the friction torque peaks were much lower than for the flat land bearing without pockets (51–55% reduction depending on the load). The measured values for that bearing design were the lowest of all the bearings under the HD mode of operation. Only slightly higher values were recorded for the pocketed bearing (12–20% higher), while the highest values of the friction torque peak were measured during tapered bearing startups.
The results suggest that the presence of the pocket has a beneficial influence on the friction torque peaks value at the startup of the fixed geometry flat land bearing under the HD mode of lubrication. This impact is similar to the case of the pocketed bearing. Both bearing designs have geometrical discontinuity of the sliding surface. The worst performance at the startup (in terms of friction torque peaks) is shown by the tapered land bearing, although that bearing design should operate the best under steady states.

4. Conclusions

A flat land thrust bearing with pockets was tested in order to perform measurements of the pressure, temperature, friction and film thickness for three modes of bearing lubrication: hydrodynamic, hydrostatic and hybrid. Pressure and temperature measurements were made both at the interface and inside the oil-jacking pockets under several operating conditions with varying speeds and static loads. As expected, it was found that the bearing has a limited load-carrying capacity regardless of the speed under the HD lubrication mode. When HS was used alone or combined with HD in the steady-state regime, the hydrostatic lift allowed the bearing to operate with an acceptable film thickness and temperature level. The speed was found to have a strong influence on the behavior of the bearing; increasing the speed led to breaking of the hydrostatic effect and the flat geometry did not allow for the creation of a hydrodynamic pressure that was strong enough to compensate for this, the oil film thickness being significantly reduced.
Transient tests of the bearing startups and stops showed significant differences in the measured parameters depending on the lubrication mode. Under HS lubrication, the bearing starts without rapid increase of the friction torque, since an oil film is already formed. It is different under HD lubrication; the friction torque peak is clearly visible just before initialization of the runner rotation and hydrodynamic film formation. However, compared to other fixed geometry bearing designs, the starting value of the friction torque peak for the bearing with pockets was very low. This is an unexpected effect and further research is necessary to understand this behavior.
As it was confirmed experimentally and theoretically, the fixed geometry flat land bearing without pockets under the HD mode of operation can support a low or average loads (up to about 1.5 MPa) [30,32]. Simultaneously, as confirmed by the present investigations, the load-carrying capacity of the same bearing design but with pockets on each pad is significantly reduced under the HD mode of lubrication. This is mainly due to the presence of hydrostatic pockets that disturb the hydrodynamic operation and contribute to thermal deformations, which are not beneficial to create a converging lubricating oil film able to generate a significant hydrodynamic pressure.

When lubricated by HS and HS+HD, the bearing can operate under full film lubrication, with a large margin of safety. This is opposite to HD lubrication, where hydrostatic pockets damage the possibility of effective hydrodynamic lubrication. In such a case, the fluid friction is limited to operation of the bearings at very low load and small speeds. Since the aim of this research was to investigate parameters under the steady state and transient operation of a flat land thrust bearing, the impact of different modes of lubrication on the dynamic bearing characteristics (stiffness and damping) was not studied.

References

[1] Bassani R, Piccigallo B, editors. Chapter 1 Hydrostatic Bearings. Hydrostatic Lubr., vol. 22, Elsevier; 1992, p. 1–14. doi:https://doi.org/10.1016/S0167-8922(08)70085-3.

[2] Osman TA, Dorid M, Safar ZS, Mokhtar MOA. Experimental assessment of hydrostatic thrust bearing performance. Tribol Int 1996. doi:10.1016/0301-679X(95)00078-I.

[3] Bassani R. Hydrostatic self-regulating multipad journal and integral bearings. Tribol Trans 2013. doi:10.1080/10402004.2012.737501.

[4] Braun MJ, Dzodzo M. Effects of hydrostatic pocket shape on the flow pattern and pressure distribution. Int J Rotating Mach 1995. doi:10.1155/S1023621X95000091.

[5] Horvat FE, Braun MJ. Comparative experimental and numerical analysis of flow and pressure fields inside deep and shallow pockets for a hydrostatic bearing. Tribol Trans 2011. doi:10.1080/10402004.2011.575535.

[6] Zhang YQ, Fan LG, Li R, Dai CX, Yu XD. Simulation and experimental analysis of supporting characteristics of multiple oil pad hydrostatic bearing disk. J Hydrodyn 2013. doi:10.1016/S1001-6058(13)60358-3.

[7] Yu X, Zuo X, Liu C, Zheng X, Qu H, Yuan T. Oil film shape prediction of hydrostatic thrust bearing under the condition of high speed and heavy load. Ind Lubr Tribol 2018. doi:10.1108/ILT-07-2017-0220.

[8] Yu X, Wang Y, Zhou D, Wu G, Zhou W, Bi H. Heat transfer characteristics of high speed and heavy load hydrostatic bearing. IEEE Access 2019. doi:10.1109/ACCESS.2019.2933471.

[9] Andrés LS, Phillips S, Childs D. A water-lubricated hybrid thrust bearing: Measurements and predictions of static load performance. J Eng Gas Turbines Power 2017. doi:10.1115/1.4034042.

[10] Childs DW, Esser P. Measurements versus predictions for a hybrid (hydrostatic plus hydrodynamic) thrust bearing for a range of orifice diameters. J Eng Gas Turbines Power 2019. doi:10.1115/1.4042721.

[11] Fesanghary M, Khonsari MM. On the optimum groove shapes for load-carrying capacity enhancement in parallel flat surface bearings: Theory and experiment. Tribol Int 2013. doi:10.1016/j.triboint.2013.08.001.

[12] Santos IF. Controllable sliding bearings and controllable lubrication principles-an overview. Lubricants 2018. doi:10.3390/lubricants6010016.

[13] Babin A, Kornaev A, Rodichev A, Savin L. Active thrust fluid-film bearings: Theoretical and experimental studies. Proc Inst Mech Eng Part J J Eng Tribol 2020. doi:10.1177/1350650119862074.

[14] Lampaert SGE, van Ostayen RAJ. Experimental results on a hydrostatic bearing lubricated with a magnetorheological fluid. Curr Appl Phys 2019;19:1441–8. doi:10.1016/j.cap.2019.09.004.

[15] Liu Z, Wang Y, Cai L, Zhao Y, Cheng Q, Dong X. A review of hydrostatic bearing system: Researches and applications. Adv Mech Eng 2017. doi:10.1177/1687814017730536.

[16] Michalec M, Svoboda P, Křupka I, Hartl M. A review of the design and optimization of large-scale hydrostatic bearing systems. Eng Sci Technol an Int J 2021. doi:10.1016/j.jestch.2021.01.010.

[17] Chaomleffel JP, Nicolas D. Experimental investigation of hybrid journal bearings. Tribol Int 1986. doi:10.1016/0301-679X(86)90004-6.

[18] De Pellegrin DV, Hargreaves DJ. An isoviscous, isothermal model investigating the influence of

hydrostatic recesses on a spring-supported tilting pad thrust bearing. Tribol Int 2012;51:25–35. doi:10.1016/j.triboint.2012.02.008.
[19] Liming Z, Yongyao L, Zhengwei W, Xin L, Yexiang X. A review on the large tilting pad thrust bearings in the hydropower units. Renew Sustain Energy Rev 2017. doi:10.1016/j.rser.2016.09.140.
[20] Wodtke M, Schubert A, Fillon M, Wasilczuk M, Pajaczkowski P. Large hydrodynamic thrust bearing: Comparison of the calculations and measurements. Proc Inst Mech Eng Part J J Eng Tribol 2014. doi:10.1177/1350650114528317.
[21] Hagemann T, Pfeiffer P, Schwarze H. Measured and predicted operating characteristics of a tilting-pad journal bearing with jacking-oil device at hydrostatic, hybrid, and hydrodynamic operation. Lubricants 2018. doi:10.3390/lubricants6030081.
[22] Heinrichson N, Fuerst A, Santos IF. The influence of injection pockets on the performance of tilting-pad thrust bearings - Part II: Comparison between theory and experiment. J Tribol 2007. doi:10.1115/1.2768610.
[23] Fillon M, Wodtke M, Wasilczuk M. Effect of presence of lifting pocket on the THD performance of a large tilting-pad thrust bearing. Friction 2015. doi:10.1007/s40544-015-0092-4.
[24] Branagan M, Morgan N, Goyne C, Fittro R, Rockwell R, He M. Hydrodynamic performance characteristics of a fluid film journal bearing with a rectangular jacking pocket. J Tribol 2020. doi:10.1115/1.4045014.
[25] Wordsworth RA, Ettles CMM. The effect of jacking pockets in hydrodynamic thrust pads. Wear 1975. doi:10.1016/0043-1648(75)90129-5.
[26] Hemmi M, Inoue T. The behavior of the centrally pivoted thrust bearing pad with hydrostatic recesses pressurized by a constant-rate flow. Tribol Trans 1999. doi:10.1080/10402009908982300.
[27] Harika E, Bouyer J, Fillon M, Hélène M. Measurements of lubrication characteristics of a tilting pad thrust bearing disturbed by a water-contaminated lubricant. Proc Inst Mech Eng Part J J Eng Tribol 2013. doi:10.1177/1350650112455783.
[28] Henry Y, Bouyer J, Fillon M. Experimental analysis of the hydrodynamic effect during start-up of fixed geometry thrust bearings. Tribol Int 2018. doi:10.1016/j.triboint.2017.12.021.
[29] Henry Y, Bouyer J, Fillon M. An experimental hydrodynamic thrust bearing device and its application to the study of a tapered-land thrust bearing. J Tribol 2014;136. doi:10.1115/1.4026080.
[30] Henry Y, Bouyer J, Fillon M. An experimental analysis of the hydrodynamic contribution of textured thrust bearings during steady-state operation: A comparison with the untextured parallel surface configuration. Proc Inst Mech Eng Part J J Eng Tribol 2015. doi:10.1177/1350650114537484.
[31] Cristea AF, Bouyer J, Fillon M, Pascovici MD. Transient Pressure and Temperature Field Measurements in a Lightly Loaded Circumferential Groove Journal Bearing from Startup to Steady-State Thermal Stabilization. Tribol Trans 2017. doi:10.1080/10402004.2016.1241330.
[32] Charitopoulos A, Fillon M, Papadopoulos CI. Numerical investigation of parallel and quasi-parallel slider bearings operating under ThermoElastoHydroDynamic (TEHD) regime. Tribol Int 2020;149. doi:10.1016/j.triboint.2018.12.017